molecular pharmaceutics

Article

pubs.acs.org/molecularpharmaceutics

Differences in Intestinal Hydrolytic Activities between Cynomolgus Monkeys and Humans: Evaluation of Substrate Specificities Using Recombinant Carboxylesterase 2 Isozymes

Yoshiyuki Igawa,[†,‡] Seiya Fujiwara,[†] Kayoko Ohura,[†] Takatsugu Hirokawa,[§] You Nishizawa,[†] Shotaro Uehara,[∥] Yasuhiro Uno,[∥] and Teruko Imai*[,†]

[†]Graduate School of Pharmaceutical Sciences, Kumamoto University, 5-1 Oe-honmachi, Chuo-ku, Kumamoto 862-0973, Japan

[‡]Drug Metabolism and Pharmacokinetics Research Laboratories, Daiichi Sankyo Co., Ltd., 1-2-58 Hiromachi, Shinagawa-ku, Tokyo 140-8710, Japan

[§]Molecular Profiling Research Center for Drug Discovery, National Institute of Advanced Industrial Science and Technology, 2-4-7 Aomi, Koto-ku, Tokyo 135-0064, Japan

[∥]Pharmacokinetics and Bioanalysis Center, Shin Nippon Biomedical Laboratories, Ltd., 16-1 Minami Akasaka, Kainan, Wakayama 642-0017, Japan

Supporting Information

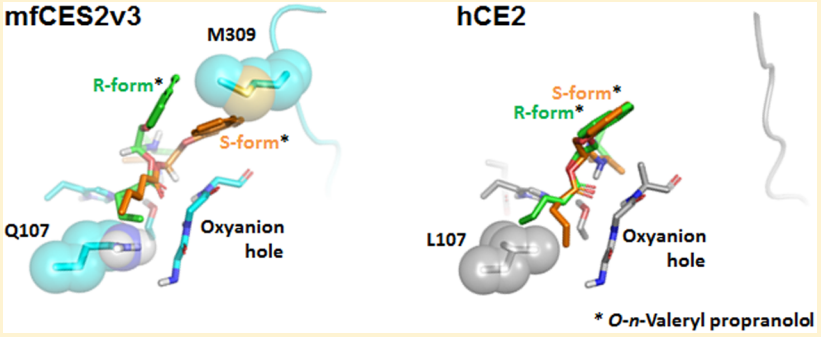

ABSTRACT: Cynomolgus monkeys, used as an animal model to predict human pharmacokinetics, occasionally show different oral absorption patterns to humans due to differences in their intestinal metabolism. In this study, we investigated the differences between intestinal hydrolytic activities in cynomolgus monkeys and humans, in particular the catalyzing activities of their carboxylesterase 2 (CES2) isozymes. For this purpose we used both human and monkey microsomes and recombinant enzymes derived from a cell culture system. Monkey intestinal microsomes showed lower hydrolytic activity than human microsomes for several substrates. Interestingly, in contrast to human intestinal hydrolysis, which is not enantioselective, monkey intestine showed preferential *R*-form hydrolysis of propranolol derivatives. Recombinant CES2 isozymes from both species, mfCES2v3 from monkeys and human hCE2, showed similar metabolic properties to their intestinal microsomes when expressed in HEK293 cells. Recombinant hCE2 and mfCES2v3 showed similar K_m values for both enantiomers of all propranolol derivatives tested. However, recombinant mfCES2v3 showed extreme *R*-enantioselective hydrolysis, and both hCE2 and mfCES2v3 showed lower activity for *O*-3-methyl-*n*-butyryl propranolol than for *O*-*n*-valeryl and *O*-2-methyl-*n*-butyryl propranolol. This lower hydrolytic activity was characterized by lower V_{max} values. Docking simulations of the protein−ligand complex demonstrated that the enantioselectivity of mfCES2v3 for propranolol derivatives was possibly caused by the orientation of its active site being deformed by an amino acid change of Leu107 to Gln107 and the insertion of Met309, compared with hCE2. In addition, molecular dynamics simulation indicated the possibility that the interatomic distance between the catalytic triad and the substrate was elongated by a 3-positioned methyl in the propranolol derivatives. Overall, these findings will help us to understand the differences in intestinal hydrolytic activities between cynomolgus monkeys and humans.

KEYWORDS: *carboxylesterase, cynomolgus monkey, small intestine, species differences, enantioselective hydrolysis, docking simulation*

INTRODUCTION

Macaques, including cynomolgus monkeys, are frequently used during both drug discovery and drug development due to their evolutionary closeness and physiological similarity to humans. Chiou and Buehler reported that the fraction dose absorbed

Received: May 4, 2016
Revised: July 3, 2016
Accepted: July 25, 2016
Published: July 25, 2016

DOI: 10.1021/acs.molpharmaceut.6b00394
Mol. Pharmaceutics 2016, 13, 3176−3186

from the gastrointestinal tract (Fa) in cynomolgus monkeys correlated well with that in humans, although bioavailability in cynomolgus monkeys was generally lower.[1] Other studies showed that the rates of oxidation by cytochrome P450 (CYP) and glucuronide conjugation by UDP-glucuronosyltransferase (UGT) were higher in cynomolgus monkey intestine than in human intestine.[2,3] It has also been reported that species differences in transporters expressed in the intestine may influence the pharmacokinetics of drugs.[4] For example, diltiazem was similarly effluxed in the small intestine by P-glycoprotein (P-gp) in both humans and cynomolgus monkeys,[5] while furosemide showed a lower bioavailability in cynomolgus monkeys than humans due to high activities of P-gp, multidrug resistance-associated protein 2 (MRP2), and breast cancer resistance protein (BCRP).[6] Thus, absorption and metabolism in monkey gastrointestinal tract may differ from that in humans, although there are some species similarities.

Carboxylesterases (CESs; EC 3.1.1.1), members of the α,β-hydrolase fold superfamily, are the major enzymes participating in the hydrolysis of various environmental toxicants, nutrients, and pharmaceutical agents containing esters or amide bonds in their structures.[7−9] Among the mammalian CES family (CES1 to CES5), human CES2 isozyme (hCE2) is predominantly present in human intestine[10,11] and is involved in the hydrolysis of several prodrugs, such as irinotecan (CPT-11)[12] and prasugrel.[13] However, when the active metabolite is to be generated from the prodrug by hCE2 in the intestine, this sometimes fails to result in the expected increase in bioavailability, due to transport of the active metabolite to the luminal side. Since hCE2 shows extremely low hydrolytic activity against substrates with relatively large acyl groups, it is theoretically possible to design a prodrug that would be minimally hydrolyzed in human intestine. Oseltamivir and temocapril are examples of successful prodrugs that are absorbed intact in intestinal mucosa and that then generate their active drugs when metabolized by human CES1 isozyme (hCE1) in the liver.[14,15]

The distinctive patterns of expression of the CES family may explain the dissimilar hydrolytic activities of human and monkey intestines, although their relative contributions to hydrolysis are unclear. Mammalian CES1 isozymes show a wide range of substrate specificities. Both CES1 and CES2 isozymes are expressed in monkey intestine.[16] Recently, Williams et al. reported the amino acid sequences of CES2 isozymes expressed in cynomolgus monkey liver and intestine[17] and demonstrated that there were some differences in hydrolytic activities between hCE2 and one of the monkey CES2 isozymes, which they designated cCES2.[18] Although we could not clone cCES2, we cloned another monkey CES2 isozyme, which we designated mfCES2v3. Quantitative polymerase chain reaction (PCR) showed mfCES2v3 to be a major CES2 transcript in several tissues, with high expression in the intestine.[19] The amino acid sequence of mfCES2v3 was found to be the same as the N-terminal sequence of another monkey CES2 isozyme (designated MK2) purified from cynomolgus monkey liver.[20] The homology of the amino acid sequence of mfCES2v3 with cCES2 was found to be 92%, suggesting that mfCES2v3 and cCES2 are similar proteins encoded by different genes. A phylogenetic tree created using the cynomolgus monkey and human CES2 amino acid sequences reported so far showed close clusters of each CES2 isozyme (Figure S1) and the monkey CES2 gene sequences identified in the genomic region corresponding to human CES2.

In this study we examined the functional differences between monkey and human intestinal hydrolysis associated with the activities of CES2 isozymes. We evaluated the hydrolytic activities using several different substrates in microsomal fractions from monkey and human intestine; the hydrolytic properties of the microsomal fractions were compared with the properties of mfCES2v3 and hCE2 recombinantly expressed in HEK293 cells. In addition, docking simulations were performed to clarify the possible mechanisms of substrate recognition of each CES2 isozyme.

MATERIALS AND METHODS

Materials. *p*-Aminobenzoic acid (PABA) derivatives were obtained from Tokyo Chemical Industry Co., Ltd. (Tokyo, Japan). *O*-Acyl-propranolol hydrochloride, previously synthesized,[21] was utilized. Pooled human small intestinal microsomes (pool of 10 subjects, PMSF-free, prepared from duodenum, jejunum, and ileum) were obtained from KAC Co., Ltd. (Shiga, Japan). Pooled cynomolgus monkey small intestinal microsomes (pool of 10 individuals, PMSF-free, prepared from duodenum and jejunum) were obtained from Xenotech, LLC (Lenexa, KS, USA). Rabbit antimonkey CES2 (MK2) and antihuman CES2 (hCE2) polyclonal antibodies were kindly provided by Dr. M. Hosokawa (Chiba Institute of Science, Chiba, Japan). Mouse anti-β-actin antibody (sc-47778) was obtained from Santa Cruz Biotechnology, Inc. (Dallas, TX, USA). All other chemicals and reagents were of analytical grade and purchased from standard commercial suppliers. The study was performed in accordance with the ethical guidelines of the Faculty of Life Sciences, Kumamoto University.

Establishment of HEK293 Cell Lines Stably Expressing Recombinant mfCES2v3 and hCE2. The cloning of mfCES2v3 was described in a previous study.[22] Similarly, hCE2 cDNA was cloned from human small intestinal total RNA by reverse transcription-PCR. The cDNA of mfCES2v3 and hCE2 was subcloned into pcDNA3.1 vector (Invitrogen, Carlsbad, CA, USA) and pTargeT vector (Promega, Madison, WI, USA), respectively. The stable HEK293 cell lines expressing recombinant mfCES2v3 and hCE2 were established by a previously described procedure.[23] Briefly, after transfection of each plasmid into HEK293 cells (American Type Culture Collection, Rockville, MD, USA; passage 10−12), the stable clones were selected by their resistance to G418. The confluent cells of stable clones were then homogenized in SET buffer (292 mM sucrose, 1 mM EDTA, and 50 mM Tris), and supernatant was collected as the S9 fraction after centrifugation (9000*g*, 4 °C, 20 min). The protein content of the S9 fraction was determined by the method described by Bradford[24] with bovine serum albumin as standard. The S9 fraction was stored at −80 °C until use. The recombinant CES isozyme content of the S9 fraction was determined with FP-biotin by the method described by Liu et al.,[25] and the content of mfCES2v3 and hCE2 in the S9 fraction was found to be 41.5 and 72.2 ng of enzyme per 2.5 μg of protein, respectively.

Western Blotting. Microsomal samples of intestines (20 μg of protein per lane) and S9 samples of HEK293 cells (2.5 μg of protein per lane) were subjected to sodium dodecyl sulfate-polyacrylamide gel electrophoresis (SDS-PAGE), and proteins were transferred to a polyvinyldifluoride (PVDF) membrane. After blocking with 5% skimmed milk in phosphate-buffered saline containing 0.05% Tween 20, the proteins on the membrane were probed with specific antibodies for human and monkey CES2 and β-actin. The membranes were

DOI: 10.1021/acs.molpharmaceut.6b00394
Mol. Pharmaceutics 2016, 13, 3176−3186

incubated with peroxidase-conjugated rabbit or mouse IgG. The immunoreactive proteins were detected by Clarity Western ECL Substrate (Bio-Rad Laboratories, Inc., Berkeley, CA, USA) using the ImageQuant LAS 4000 (GE Healthcare Life Sciences, Piscataway, NJ, USA).

***In Vitro* Hydrolytic Reactions.** Enzyme solutions (intestinal microsomes or S9 fractions of HEK293 cells) were diluted to the appropriate concentration with 50 mM HEPES buffer, pH 7.4. After preincubation at 37 °C for 5 min, each hydrolytic reaction was initiated by the addition of propranolol derivatives (final concentration 2.5−50 μM) or PABA derivatives (final concentration 500 μM) dissolved in dimethyl sulfoxide (DMSO). The final concentration of DMSO in the reaction mixture was less than 1%, which had no effect on hydrolytic activity. The reaction time was set to be below 20% hydrolysis. For hydrolysis of PABA derivatives, the reaction was terminated by addition of ice-cold methanol. After centrifugation, the supernatant was added to phosphoric acid (final concentration 25 mM) and then analyzed by high performance liquid chromatography (HPLC). For hydrolysis of propranolol derivatives, the reaction was terminated by addition of ethyl acetate and saturated NaCl solution adjusted to pH 4 with phosphoric acid. After shaking for 10 min, the mixture was centrifuged and the ethyl acetate phase isolated and evaporated. The residue was redissolved in hexane/2-propanol, 4:1 (v/v), and analyzed by HPLC. Hydrolytic activity was represented as the nanomole or micromole of hydrolysate per minute per milligram of microsomal or recombinant CES proteins. The activities of recombinant samples were calculated by subtraction of the activities of S9 fractions derived from mock-infected HEK293 cells.

Quantitative Analysis of Metabolites by HPLC. The HPLC system consisted of a Jasco PU-2089 pump Jasco AS-2055 plus autosampler, Jasco CO-965 column oven, and Jasco FP-1520S fluorescence detector, and the data was analyzed by Jasco ChromNAV (all Jasco International Co. Ltd., Tokyo, Japan). The column oven was set at 40 °C. For measurement of PABA, Inertsil ODS-2 (250 mm × 4.6 mm ID, 5 μm; GL Sciences, Inc., Tokyo, Japan) was used with mobile phase (0.1% phosphoric acid/acetonitrile, 80:20) at a flow rate of 1.0 mL/min. PABA was detected by fluorescence at excitation and emission wavelengths of 291 and 330 nm, respectively. For measurement of propranolol, Chiralcel OD (250 mm × 4.6 mm ID, 10 μm; Daicel Corp., Osaka, Japan) was used with mobile phase (hexane/2-propanol/diethylamine, 90:10:0.5) at a flow rate of 1.0 mL/min. Propranolol was detected by fluorescence at excitation and emission wavelengths of 285 and 340 nm, respectively. All substrates and hydrolysates were clearly separated, and each hydrolysate was measured in a quantitatively linear range.

Data Analysis. Experimental reaction velocity results are presented as the mean ± SD values. The K_m and V_{max} values were calculated by the Michaelis−Menten equation using nonlinear regression analysis (MULTI, Gauss−Newton method).[26] Intrinsic clearance was calculated by dividing V_{max} by K_m.

Homology Modeling of hCE2 and mfCES2v3. The hCE2 and mfCES2v3 sequences were aligned with the known structural hCE1 sequence (Protein Data Bank ID: 2DQY)[27] using MOE ver. 201402 (Chemical Computing Group, Quebec, Canada). The alignment was refined manually on the basis of the compatibility of the amino acid positions with the corresponding structure of hCE1 (Figure S2). Three-dimensional models of hCE2 and mfCES2v3 were constructed using a homology modeling approach incorporated in Prime (Schrödinger LLC, New York) using the default parameters.

Docking and Molecular Dynamics Simulation. Initial coordinates of all compounds were constructed using the Molecular Builder module in Maestro (Schrödinger LLC). Energy minimization of all compounds was performed using LigPrep in Maestro. The homology models of hCE2 and mfCES2v3 were refined for docking simulations using the Protein Preparation Wizard Script within Maestro. Docking of the compounds into the hCE2 and mfCES2v3 models utilized two steps: (1) docking of compounds into the active sites of hCE2 and mfCES2v3 by Glide SP mode (Schrödinger LLC),[28] up to 100 poses per compound, and (2) the best pose for each docked compound was rescored according to the sum of three distances: first between Ser228 O^{γ} and the carbonyl carbon atom of the compound, second between the hydrogen atom of the backbone NH group of Gly149 and the carbonyl oxygen atom of the compound, and third between the hydrogen atom of the backbone NH group of Ala150 (hCE2) or Gly150 (mfCES2v3) and the carbonyl oxygen atom of the compound.

The final models of hCE2 and mfCES2v3 with docked compounds were subjected to 20 ns molecular dynamics (MD) simulation using the program Desmond ver. 3.4.0.1[29] for the analysis of distance profiles between Ser228 O^{γ} and the carbonyl carbon atoms of the two *R*-form propranolol derivatives. The OPLS2005 force field was used for the simulations. Initial model structures were placed into TIP3P water molecules solvated with 0.15 mol/L NaCl. After minimization and relaxation of the model, the production MD phase was performed for 20 ns in the isothermal−isobaric (NPT) ensemble at 300 K and one bar using Langevin dynamics. Long-range electrostatic interactions were computed using the Smooth Particle Mesh Ewald method. All system setups were performed using Maestro.

RESULTS

Confirmation of Recombinant CES2 Expression in HEK293 Cells and Presence of CES2 in Intestinal Microsomes. Figure 1A shows the Western blot of human and monkey intestinal microsomes using monkey anti-MK2 polyclonal antibody. Although there were two bands that reacted with the anti-MK2 antibody in cynomolgus monkey intestine, the upper band was assigned to mfCES2v3 based on its mobility. The lower band is an unknown CES2 isozyme. The anti-MK2 polyclonal antibody was able to react with hCE2 due to its high amino acid sequence similarity. Interestingly, human intestinal microsomes showed an intense band due to the high expression of hCE2.

The recombinant hCE2 and mfCES2v3 were expressed in HEK293 cells, and their S9 samples were subjected to immunoblotting analysis with anti-hCE2 and anti-MK2 polyclonal antibodies. As shown in Figure 1B,C, bands of hCE2 and mfCES2v3 were detected with both anti-hCE2 and anti-MK2 antibodies, although hCE2 and mfCES2v3 reacted more strongly with anti-hCE2 antibody and anti-MK2 antibody, respectively. Their bands were at molecular weight positions 61 and 63 kDa, respectively. Immunoblotting was repeated more than three times, and the band density was comparable in all experiments.

Comparison of Hydrolytic Characteristics of Intestinal Microsomes in Monkeys and Humans with Those of CES2 Isozymes, mfCES2v3, and hCE2. Hydrolytic activity was evaluated using two types of substrate consisting of

DOI: 10.1021/acs.molpharmaceut.6b00394
Mol. Pharmaceutics 2016, 13, 3176−3186

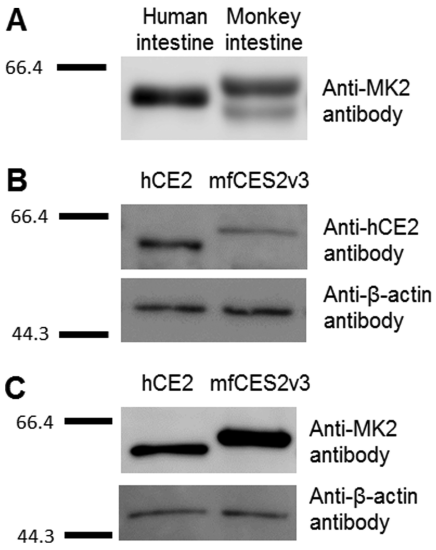

Figure 1. Confirmation of CES2 protein expressions by Western blot analysis. (A) Representative results for cynomolgus monkey and human intestinal microsomes using anti-MK2 antibody. A microsomal sample of 20 μg of protein was applied in each lane. (B) Representative results for S9 samples of mfCES2v3- or hCE2-expressing HEK293 cells using anti-hCE2 antibody and anti-β-actin antibody. An S9 sample of 2.5 μg of protein was applied in each lane. (C) Representative results for S9 samples of mfCES2v3- or hCE2-expressing HEK293 cells using anti-MK2 antibody and anti-β-actin antibody. An S9 sample of 2.5 μg of protein was applied in each lane.

different-sized acyl and alcohol groups. For PABA ester derivatives, the carbonyl group of PABA was substituted with the small alcohol groups, methyl (C1), ethyl (C2), propyl (C3), and butyl (C4) esters (summarized structures are shown in Figure 2; detailed steric structures in Supporting Figure S3). The propranolol ester derivatives consisted of several different small acyl groups with propranolol as a large alcohol group (summarized structures are shown in Figure 3; detailed steric structures in Supporting Figure S3).

Hydrolysis of PABA Derivatives by Intestinal Microsomes from Monkeys and Humans. Hydrolysis of PABA derivatives was studied in monkey intestine and compared with that in human intestine (Figure 2A,B). The hydrolase activity of small intestine was evaluated as an average of the overall intestine, including the jejunum and ileum. Monkey intestinal hydrolysis required an alcohol carbon chain (Figure 2A). When the two species were compared, the hydrolytic activities of monkey intestinal microsomes for C1, C2, C3, and C4 were 1.6, 5.1, 3.0, and 2.7 times lower, respectively, than those of human intestine, indicating that intestinal hydrolysis in monkeys is lower than in humans for all four PABA derivatives. Hydrolysis of PABA derivatives by monkey and human intestinal microsomes was more than 90% inhibited by addition of a high concentration (500 μM) of bis-*p*-nitrophenylphosphate (BNPP), a potent CES inhibitor[31] (unpublished data), indicating that CES is the major esterase for hydrolysis of PABA derivatives in both monkey and human intestine.

Hydrolysis of PABA Derivatives by Recombinant mfCES2v3 and hCE2. The hydrolytic activities of recombinant mfCES2v3 and hCE2 for PABA derivatives are also shown in Figure 2C,D. The derivatives with longer alcohol chains were highly hydrolyzed by the recombinant enzymes (mfCES2v3 and hCE2) as well as by intestinal microsomes. However, the hydrolytic rates of methyl (C1) and ethyl (C2) esters of PABA by recombinant hCE2 were extremely low in comparison with human intestinal microsomes. In contrast, the effect of alcohol chain length on hydrolysis of PABA derivatives by recombinant mfCES2v3 was relatively similar to that found in monkey intestine, even though several CES1 and CES2 isozymes are present in monkey intestinal microsomes (Figure S4).

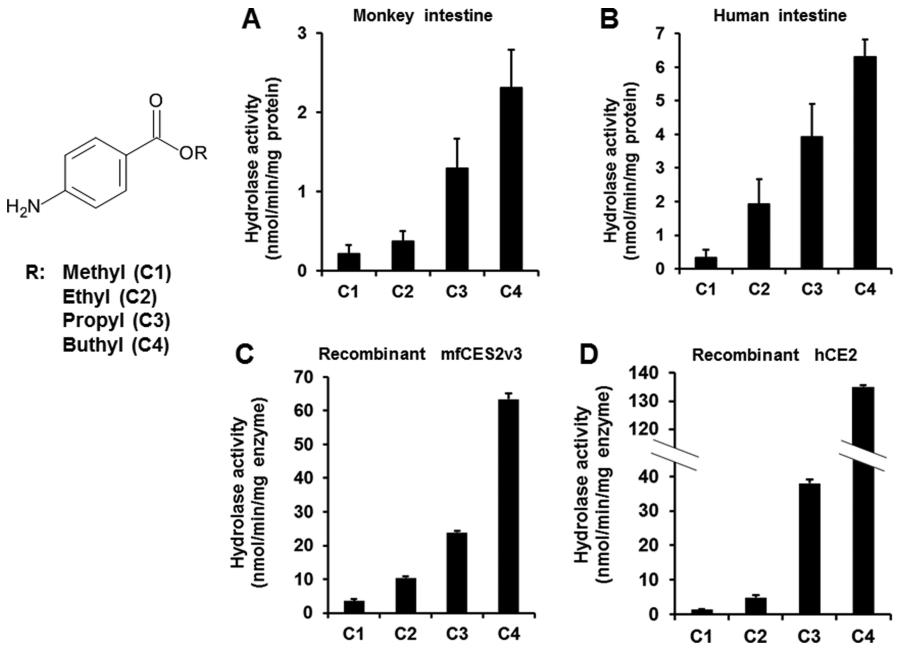

Figure 2. Chemical structures and hydrolytic activities for PABA derivatives. For four types of PABA derivatives with different lengths of carbon chain in the alcohol moiety (C1 to C4), *in vitro* hydrolytic activities with intestinal microsomes of (A) monkey or (B) human and S9 samples of (C) mfCES2v3- or (D) hCE2-expressing HEK293 cells were examined. The final concentration of microsomal and S9 protein was set to be 100 μg/mL at the time of the reaction. The data represent means ± SD.

DOI: 10.1021/acs.molpharmaceut.6b00394
Mol. Pharmaceutics 2016, 13, 3176−3186

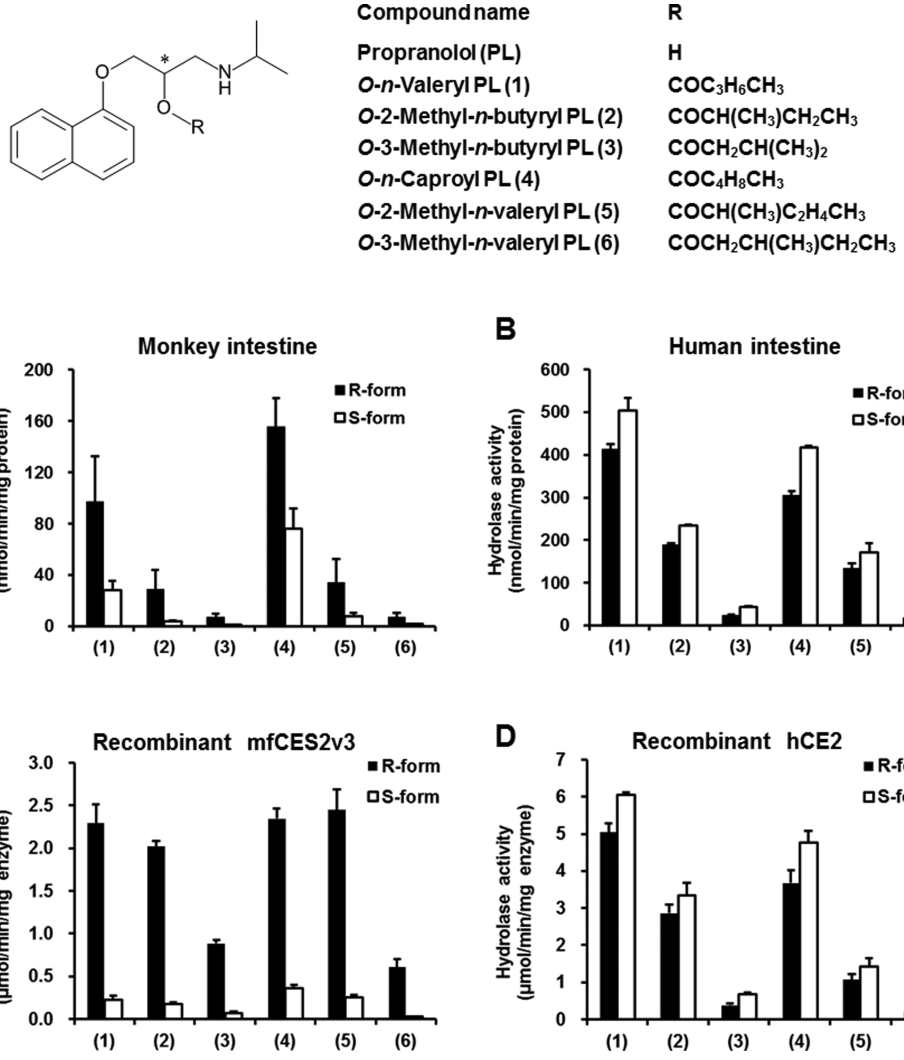

Figure 3. Chemical structures and hydrolytic activities for propranolol derivatives. The asterisk (*) in the structure shows an asymmetric carbon. Twelve derivatives were tested, with acyl moieties in six different structures represented as (1) to (6) and both *R*- and *S*-forms for each structure. *In vitro* hydrolytic activities were examined with intestinal microsomes of (A) monkey or (B) human and S9 samples of (C) mfCES2v3- or (D) hCE2-expressing HEK293 cells. The final concentration of microsomal and S9 protein was set to be 20−40 μg/mL at the time of the reaction. The data represent means ± SD.

Hydrolysis of Propranolol Derivatives by Intestinal Microsomes from Monkeys and Humans. Propranolol derivatives with acyl moieties consisting of 4 or 5 carbon atoms were substituted by methyl groups at 2-, 3-, and the terminal carbon of the acyl group. Hydrolytic activities for propranolol derivatives were measured stereoselectively. These *in vitro* hydrolyses of propranolol derivatives were nearly completely inhibited by the addition of 500 μM BNPP in both human and monkey intestinal microsomes (unpublished data), indicating that these derivatives are mainly hydrolyzed by CES. Higher activities were observed in human than monkey intestine for all propranolol derivatives tested (Figure 3A,B). In both monkeys and humans, metabolizing velocity increased in the order: straight chain derivatives, 2-methylated acyl derivatives, and 3-methylated acyl derivatives ((1) > (2) > (3) and (4) > (5) > (6)). Interestingly, the hydrolase activities of human intestinal microsomes were nearly the same with *R*- and *S*-enantiomers, whereas monkey intestinal microsomes predominantly hydrolyzed *R*- rather than *S*-forms.

Hydrolysis of Propranolol Derivatives by Recombinant mfCES2v3 and hCE2. The hydrolase activities of recombinant mfCES2v3 and hCE2 for propranolol derivatives are also shown in Figure 3C,D. Recombinant hCE2 showed nearly equal hydrolysis of *R*- and *S*-forms of all propranolol derivatives and a lower activity for derivatives with a branched acyl chain, especially the 3-methylated acyl chain. The profile of hCE2 hydrolytic activities for propranolol derivatives corresponded totally with that for human intestinal activity, suggesting that hCE2 plays a major role in the hydrolysis of propranolol derivatives in human intestine. In contrast, recombinant mfCES2v3 showed different structural requirements with respect to the acyl group of propranolol derivatives from monkey intestinal microsomes. The hydrolytic velocities of mfCES2v3 were comparable for straight-chain and 2-methylated acyl derivatives, but 3-methylated acyl derivatives were more slowly hydrolyzed. In addition, the hydrolysis of mfCES2v3 showed marked *R*-enantioselectivity, with activities for *R*-forms 6.5- to 21.8-fold greater than those for *S*-forms. These characteristics were completely different from those of hCE2, indicating dissimilar substrate recognition requirements. Furthermore, the different structural requirements for hydrolysis of recombinant mfCES2v3 and monkey intestine with

DOI: 10.1021/acs.molpharmaceut.6b00394
Mol. Pharmaceutics 2016, 13, 3176−3186

Table 1. Kinetic Parameters of *O*-*n*-Valeryl Propranolol, *O*-2-Methyl-*n*-butyryl Propranolol, and *O*-3-Methyl-*n*-butyryl Propranolol Hydrolysis by S9 Samples of Recombinant mfCES2v3- and hCE2-Expressing HEK293 Cells[a]

compd	enzyme	configuration of isomer	K_m (μM)	V_{max} (nmol/min/mg enzyme)	CL_{int} (mL/min/mg enzyme)
O-*n*-valeryl propranolol	hCE2	*R*-isomer	12.0 ± 4.9	5135.5 ± 251.4	459.9 ± 165.1
		S-isomer	17.8 ± 8.4	7577.2 ± 1104.9	461.5 ± 155.1
	mfCES2v3	*R*-isomer	10.6 ± 1.4	2675.6 ± 409.2	258.3 ± 73.6
		S-isomer	6.6 ± 1.4	263.8 ± 89.9	42.7 ± 22.9
O-2-methyl-*n*-butyryl propranolol	hCE2	*R*-isomer	12.5 ± 1.4	3217.4 ± 62.3	259.0 ± 24.9
		S-isomer	14.9 ± 0.9	3966.9 ± 9.2	266.5 ± 15.7
	mfCES2v3	*R*-isomer	13.2 ± 0.3	3012.8 ± 31.7	228.3 ± 3.4
		S-isomer	4.5 ± 0.1	230.8 ± 3.4	50.8 ± 0.5
O-3-methyl-*n*-butyryl propranolol	hCE2	*R*-isomer	2.4 ± 0.3	341.1 ± 40.7	142.9 ± 37.0
		S-isomer	4.0 ± 2.0	668.1 ± 103.6	186.4 ± 69.3
	mfCES2v3	*R*-isomer	7.2 ± 2.4	891.4 ± 8.4	131.1 ± 45.3
		S-isomer	9.0 ± 4.2	66.6 ± 8.1	8.0 ± 2.8

[a]Values represent means ± SD.

respect to the acyl moiety, point to the contributions of several hydrolases in monkey intestine, such as CES1 and other CES2 isozymes.

Determination of *in Vitro* Kinetic Parameters for Propranolol Derivatives. To clarify the differences between mfCES2v3 and hCE2 with respect to substrate recognition, the kinetic parameters for *R*- and *S*-forms of *O*-*n*-valeryl, *O*-2-methyl-*n*-butyryl, and *O*-3-methyl-*n*-butyryl propranolol were determined. The kinetic parameters (K_m, V_{max}, and CL_{int}) are listed in Table 1. The kinetic parameters of hCE2 were similar for *R*- and *S*-forms of each compound. In mfCES2v3, the K_m values of *S*-form derivatives were either a little smaller or nearly the same as those of *R*-form derivatives, while V_{max} values were much smaller for *S*-forms than *R*-forms for all substrates. Therefore, the *R*-preferential hydrolysis by mfCES2v3 cannot be attributed to affinity but depends on V_{max}. Interestingly, *O*-3-methyl-*n*-butyryl propranolol was hydrolyzed by both hCE2 and mfCES2v3 at the lowest rate. The K_m and V_{max} values of *O*-3-methyl-*n*-butyryl propranolol indicate that it is probably bound to CES2 isozymes but that its hydrolysis does not proceed. These data suggest that the differences in activity toward acyl chain structures and enantioselectivity between mfCES2v3 and hCE2 are derived from differences in V_{max}, not the affinities of the substrates for the enzymes.

Docking Simulations of CES2 and Propranolol Derivatives. To investigate the cause of the enantioselectivity of mfCES2v3, the steric conformation of its protein−ligand complex was examined using docking simulations. A typical docking model of hCE2 and the *R*-form of *O*-*n*-valeryl propranolol was constructed based on crystal information on hCE1. As shown in Figure 4, the acyl−enzyme complex in the model was stabilized by two hydrogen bonds with distances of 3.1 and 2.4 Å between the carbonyl oxygen atom of *O*-*n*-valeryl propranolol and the hydrogen atoms on the amide nitrogen of the oxyanion hole, Gly149 and Ala150, respectively, in hCE2. The O^{γ} atom of Ser228 in the catalytic triad was 3.1 Å apart from the ester bond carbon of *O*-*n*-valeryl propranolol, so it could attack the substrate for hydrolysis. A docking model for the *S*-form of *O*-*n*-valeryl propranolol was also constructed, resulting in a similar configuration to that of the *R*-form. The distances of the carbonyl oxygen on the *S*-form from Gly149 and Ala150 of hCE2 were 2.9 and 2.4 Å, respectively, in the docking model, and the distance between the Ser228 O^{γ} atom and the carbonyl carbon on the *S*-form was 3.1 Å.

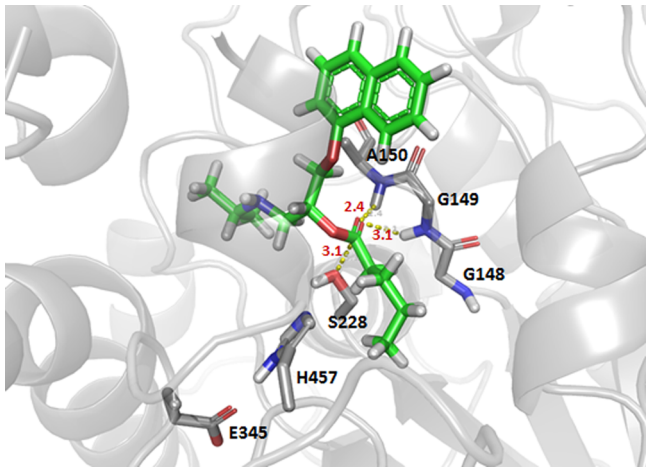

Figure 4. Predicted model of hCE2 binding with the *R*-form of *O*-*n*-valeryl propranolol using homology modeling with the crystal structure of hCE1 and docking simulation. The catalytic triad (Ser228, His457, and Glu345) and the oxyanion hole (Gly149 and Ala150) in hCE2 are depicted in sticks. The distances (Å) between the oxygen atom of Ser228 and the carbonyl carbon atom of the substrate, and the hydrogen atoms of the oxyanion hole (Gly149 and Ala150) and the carbonyl oxygen atom of the substrate are shown in the structure of the docking model.

In Figure 5, by overlapping the estimated structures of mfCES2v3 and the hCE2−substrate complex model, two amino acids in the active sites of mfCES2v3 and hCE2 were found to be different; the Leu107 in hCE2 is converted to Gln107 in mfCES2v3, and Met309 is inserted in mfCES2v3. Conversion of a hydrophobic amino acid (Leu) to a hydrophilic amino acid (Gln) diminishes the spatial freedom of the propranolol derivatives in mfCES2v3, while the insertion of Met309 influences the size of the active site pocket, leading to steric hindrance for complexation with a substrate.

Figure 6 shows the results of the docking simulations of mfCES2v3 and hCE2 for *R*- and *S*-forms of *O*-*n*-valeryl propranolol. In the model, the hydrophilic side-chain of Gln107 in mfCES2v3 represents a repulsive force against the valeryl ester of the substrate, resulting in the naphthyl group of the *S*-form substrate being close to Met309. This suggests that the hydrolysis of the *S*-form is suppressed by steric hindrance. In contrast, the naphthyl group of the *R*-form was able to avoid steric hindrance with Met309 in the docking structure. In the

DOI: 10.1021/acs.molpharmaceut.6b00394
Mol. Pharmaceutics 2016, 13, 3176−3186

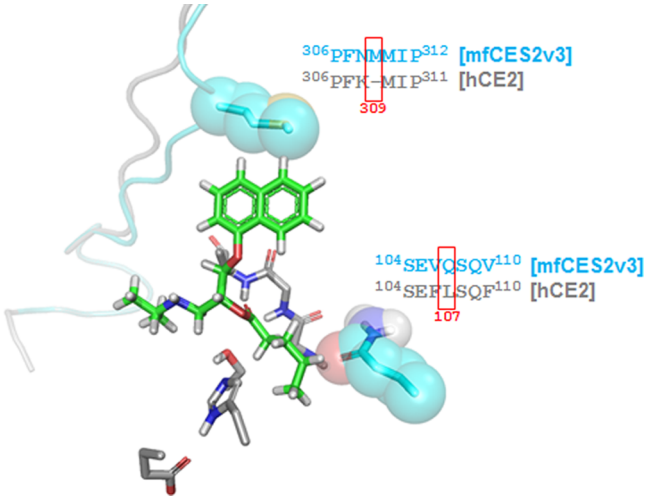

Figure 5. Active sites of mfCES2v3 superimposed on the docking model of hCE2 and *R*-form of *O*-*n*-valeryl propranolol showing the adjacent amino acids between mfCES2v3 (in cyan) and hCE2 (in gray). The basic construction of mfCES2v3 was similar to hCE2, but the insertion of Met309 in mfCES2v3 diminishes the space of the active site. In addition, Leu107, which is close to the acyl carbon chain in propranolol derivatives, is converted to the hydrophobic amino acid, Gln107. Balloon atoms represent side chains of Met309 and Gln107 in mfCES2v3.

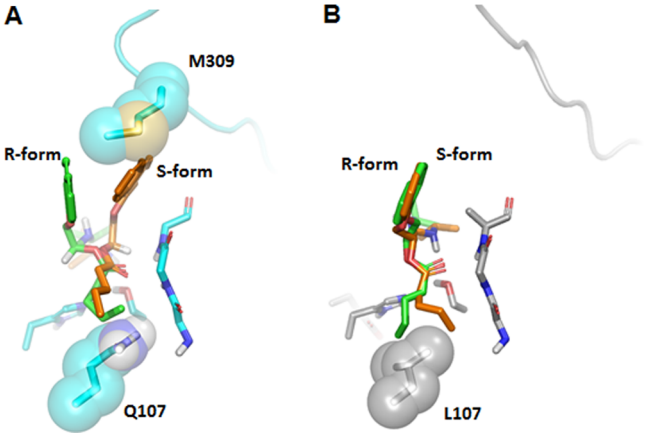

Figure 6. Docking models around active sites showing the binding conformation between mfCES2v3 (A) or hCE2 (B) and *O*-*n*-valeryl propranolol (*R*-form in green and *S*-form in orange). Balloon atoms represent side-chains of Met309 and Gln107 in mfCES2v3, and Leu107 in hCE2.

case of hCE2, Leu107, with a hydrophobic side-chain, does not restrict the interaction with *O*-*n*-valeryl propranolol. Moreover, it is possible that the absence of a Met gives the active site enough space to allow the same hydrolytic activities for *R*- and *S*-forms.

The docking simulation also sheds light on the different hydrolytic velocities, which depend on the position of the substituted methyl group on the acyl moiety released from the propranolol derivatives. As shown in Table 1, *O*-3-methyl-*n*-butyryl propranolol was less hydrolyzed in both mfCES2v3 and hCE2 than either *O*-*n*-valeryl or *O*-2-methyl-*n*-butyryl propranolol. In particular, a large difference in velocity was observed between the hydrolyses of *O*-*n*-valeryl and *O*-3-methyl-*n*-butyryl propranolol by hCE2. Their complexes with hCE2 were therefore analyzed by MD simulation. Figure 7 shows the

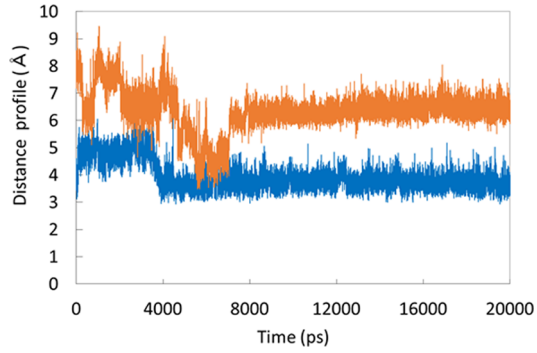

Figure 7. Distance profiles between the oxygen atom in Ser228 of the catalytic triad in hCE2 and the carbonyl carbon atoms in *R*-forms of *O*-*n*-valeryl propranolol (plotted in blue) or *O*-3-methyl-*n*-butyryl propranolol (plotted in orange) during the MD calculation. Snapshots were taken every picosecond during the 20 ns production phase.

distance profiles between the Ser228 O^{γ} atom in hCE2 and the electrophilic carbonyl carbon atoms of the two *R*-form propranolol derivatives. The results indicated that the interatomic distance of *O*-*n*-valeryl propranolol, which remained 3−4 Å after 4 ns, was shorter than that of *O*-3-methyl-*n*-butyryl propranolol, which remained 6−7 Å after 7 ns. The differences in the distance between the catalytic triad and the substrate during the stable phase may influence the hydrolytic velocities for the two propranolol derivatives.

DISCUSSION

Previously, we reported that several CES1 and CES2 isozymes are expressed in cynomolgus monkey intestine, while only hCE2 is expressed in human intestine (Figure S4).[16,30] In this study, the hydrolytic activities of monkey and human intestines were compared, and the possible contribution of mfCES2v3 to monkey intestinal hydrolysis was examined under standardized *in vitro* conditions. The homology of the amino acid sequences of mfCES2v3 and hCE2 is 89%, and they have a different total number of amino acid residues,[19] with mfCES2v3 having two additional amino acids, Met309 and Lys547. Like hCE2, mfCES2v3 is expressed as a monomer; it has an isoelectric point of 4.3, which is similar to that of hCE2 (4.7).[20] When examining the hydrolytic activities of intestinal samples, it was decided to use microsomal fractions since CES is mainly expressed in the endoplasmic reticulum of cells.[20]

In order to compare the intrinsic activities of mfCES2v3 and hCE2, the S9 samples of HEK293 expressing the respective CES2 isozymes were used as an enzyme source to obtain greater amounts of recombinant CES isozymes. Two types of substrate were selected for functional analyses of CES isozymes because the relative sizes of the acyl and alcohol moieties in substrates are important for the substrate specificity of the CES isozymes. As shown in previous studies using hCE1 and hCE2, hCE2 hardly hydrolyzes substrates with relatively large acyl groups, while extensively hydrolyzing substrates with relatively large alcohol groups.[14,15,32] Regarding the substrates used in this study, PABA derivatives with small alcohols are poor substrates for hCE2 so the length of the alcohol chain was changed. Propranolol derivatives, however, are good substrates for hCE2 due to the large alcohol group, and we utilized derivatives with various acyl chains.

The results of the *in vitro* hydrolytic reactions indicated that the hydrolyses of PABA and propranolol derivatives were faster in human intestine than in monkey intestine. The cause of this

DOI: 10.1021/acs.molpharmaceut.6b00394
Mol. Pharmaceutics 2016, 13, 3176−3186

may be the high expression levels and hydrolytic activities of hCE2 in human intestine. Our previous studies have demonstrated that hCE2 hardly hydrolyzes PABA derivatives with short alcohol chains and that its activity increases with alcohol chain length, while hydrolysis by hCE1, a human CES1 isozyme, was slower for PABA derivatives with long alcohol chains.[21] The present results for hCE2 support our previous data, and the hydrolytic profile of mfCES2v3 was shown to be similar to that of hCE2. In a comparison of the hydrolytic activities of mfCES2v3 and hCE2, we concluded that PABA derivatives with shorter alcohols (C1 and C2) are better substrates for mfCES2v3 than hCE2, while derivatives with longer alcohols (C3 and C4) were better substrates for hCE2 than mfCES2v3. It seems that this dominant characteristic of hCE2, of minimally hydrolyzing substrates with relatively large acyl groups, is less strong in mfCES2v3. The results of our experiments using recombinant CES2 isozymes suggest a significant contribution of CES2 isozymes to intestinal hydrolyses in both species, as shown in Figure 2. Interestingly, monkey intestinal hydrolysis of PABA derivatives was similar to that of recombinant mfCES2v3, in spite of the presence of CES1 and other CES2 isozymes in monkey intestines. However, the hydrolytic profiles of PABA derivatives in human intestinal microsomes were a little different from those using recombinant hCE2; that is, PABA derivatives with short alcohol chains were more extensively hydrolyzed than would be predicted from the activity of recombinant hCE2. Although BNPP, a potent inhibitor of CES, mostly inhibited the intestinal hydrolyses of PABA derivatives, carboxymethylenebutenolidase, which is present in human intestine as a major esterase for olmesartan medoxomil, was also inhibited by BNPP.[33] Therefore, several unknown esterases that are inhibited by BNPP may be involved in human intestinal hydrolysis of PABA derivatives with very short alcohols, such as methanol and ethanol.

However, human intestinal hydrolysis of propranolol derivatives, typical substrates for hCE2, showed profiles comparable to recombinant hCE2. In contrast to the nearly equal hydrolysis of *R*- and *S*-forms of propranolol derivatives by hCE2, mfCE2v3 preferentially hydrolyzed the *R*-forms of propranolol derivatives. The ratio of the hydrolytic activities of *R*-form to *S*-form propranolol derivatives (*R*/*S*-form) was different between recombinant mfCES2v3 and monkey intestinal microsomes. The *R*/*S*-form ratios for hydrolysis of compounds (1) and (4) were both approximately 2:1 in monkey intestinal microsomes, but 10:1 and 7:1 in recombinant mfCES2v3, respectively. The ratios of other propranolol derivatives with branched acyl chains were comparable using intestinal microsomes and recombinant mfCES2v3. These data suggest that other CES isozymes, including CES1 and other CES2 isozymes, in addition to mfCES2v3, may be involved in the hydrolysis of straight-chain derivatives of propranolol in monkey intestine.

Overall, analysis of the hydrolysis of PABA and propranolol derivatives showed that mfCES2v3 significantly contributes to monkey intestinal hydrolysis. Interestingly, mfCES2v3 enantioselectively catalyzed the hydrolysis of propranolol derivatives in comparison with the nonenantioselective hydrolysis by human hCE2. The kinetic parameters indicate that *R*- and *S*-forms of propranolol derivatives interacted with mfCES2v3 to a nearly equal extent, but their different maximum velocities contribute to their enantioselective hydrolysis.

In order to clarify the causes of the difference in enantioselective hydrolysis of propranolol derivatives between mfCES2v3 and hCE2, we studied the conformation of the enzyme−substrate complex using docking simulation. Regarding the crystal structures of carboxylesterases, diffraction data of purified rabbit CES1 was the first to be reported;[34] thereafter, the protein structures and conformations of several substrates for hCE1 have been reported.[35−38] However, the conformation of hCE2 has not been reported because of difficulties in conducting crystal analysis due to the low stability of the purified hCE2 protein,[39] although homology modeling of hCE2 predicted from the structure of hCE1 has previously been reported.[40] In addition, there have so far been no reports about the conformation of monkey CES. Therefore, the structures of mfCES2v3 and hCE2 were predicted based on hCE1 construction, and docking simulations were conducted using their estimated structures.

Docking simulations demonstrated that changes in two amino acids around the active center led to the distinct substrate specificities of hCE2 and mfCES2v3; namely, the conversion of Leu107 in hCE2 to Gln107 in mfCES2v3 and the insertion of Met309 in mfCES2v3. These conversions seem to have induced changes in the size and orientation of the active site, resulting in markedly slower hydrolytic rates of *S*-*n*-valeryl propranolol by mfCES2v3. As shown in Figure 6A, the naphthyl group in the *S*-form of *O*-*n*-valeryl propranolol is very close to the Met309, and this tightness may make the hydrolytic reaction difficult. The cause of this closeness is considered to be a repulsive force between the hydrophilic side chain of Gln107 in mfCES2v3 and the hydrophobic valeryl moiety of the substrate, which only occurs in the *S*-form. Comparable K_m values for the *R*- and *S*-forms indicate that, in both cases, the substrate is present in the active center of mfCES2v3. We suggest that hydrolysis of the *S*-form may be more difficult to achieve due to steric hindrance. Meanwhile, hCE2 did not show enantioselective hydrolysis of propranolol derivatives. The hydrophobic amino acid Leu107 in hCE2 may not induce the same repulsive interaction with the propranolol derivatives, resulting in the formation of similar complexes with both *R*- and *S*-forms, as described in a previous study.[40] The major reason for the difference of enantioselectivity in the hydrolysis of propranolol derivatives between monkey and human CES2 isozymes may therefore be the conversion of the two amino acids (Gln107 and Met309). The importance of Gln107 and/or Met309 for the hydrolytic activities of mfCES2v3 will be further investigated using point mutations in the future.

Generally, substitution of a methyl group in the releasing acyl moiety affects hydrolysis. In chemical hydrolysis, 2-methyl acyl shows low hydrolysis due to limitation of the attack by the hydroxyl group because of steric hindrance. However, both mfCES2v3 and hCE2 show significantly slower hydrolysis of *O*-3-methyl-*n*-butyryl derivatives in comparison with *O*-2-methyl-*n*-butyryl derivatives. In addition, low hydrolytic activity for *O*-3-methyl-*n*-butyryl derivatives was observed even in hCE2 with its wide active-site pocket. These phenomena led us to consider the possibility of *O*-3-methyl-*n*-butyryl propranolol being a CES2-specific inhibitor since hCE1 showed nearly the same levels of hydrolysis with three propranolol derivatives substituted with a methyl group at different positions in the acyl moiety.[21] Therefore, we decided to compare the different hydrolytic activities of hCE2 with the two propranolol derivatives, *O*-*n*-valeryl and *O*-3-methyl-*n*-butyryl propranolol,

DOI: 10.1021/acs.molpharmaceut.6b00394
Mol. Pharmaceutics 2016, 13, 3176−3186

using docking simulation. For the potency of hydrolysis by CES, the determinants are the distances between key atoms of the enzyme and the ligand; between the O^{γ} atom of Ser228 in the catalytic triad in the enzyme and the carbonyl carbon atom of the substrate, and between the amide nitrogen atoms of the oxyanion hole in the enzyme and the carbonyl oxygen atom of the substrate. In the preliminary analysis, distances between these atoms in the docking models were confirmed to be comparable for *O*-*n*-valeryl and *O*-3-methyl-*n*-butyryl propranolol. K_m values of these propranolol derivatives for hCE2 were also comparable (Table 1), indicating that both substrates could bind to the active-site pocket of the enzyme.

During the MD simulations of the docking models, the atoms fluctuated and the distances of atoms were changed in the enzyme−ligand complexes. The distances between the oxyanion hole and the carbonyl oxygen atom of the substrates were similar in *O*-*n*-valeryl and *O*-3-methyl-*n*-butyryl propranolol, even in the MD simulation. However, the distance between the O^{γ} of Ser228 in the catalytic triad of hCE2 and the carbonyl carbon atom of a propranolol derivative in the docking model was shorter in *O*-*n*-valeryl propranolol than in *O*-3-methyl-*n*-butyryl propranolol (Figure 7). This difference during the MD simulation may have had an impact on the V_{max} values of hydrolysis, which correspond with the results of *in vitro* enzymatic kinetic analysis of the hydrolysis of propranolol derivatives. In addition, the inhibitory experiments with mfCES2v3 and hCE2 demonstrated that pre- and simultaneous treatment with *O*-3-methyl-*n*-butyryl propranolol showed comparable levels of inhibition of the hydrolysis of *p*-nitrophenyl acetate, indicating competitive inhibitory effects (Figure S5). These data suggest that *O*-3-methyl-*n*-butyryl propranolol can enter the active site of CES2 isozymes and can also be easily released by substitution with other compounds.

In this study, it has been shown that docking and MD simulation of the detailed conditions around the active site of CES2 can explain differences in the hydrolytic activities of human and monkey CES2 isozymes. Docking and MD simulation analysis based on estimated structures may therefore be a powerful tool in improving our understanding of enzymatic substrate specificity.

Recently, Williams et al. reported on a new monkey CES2 (cCES2) isolated from cynomolgus monkey intestine.[18] cCES2 has a very similar amino acid sequence (92%) to mfCES2v3. Figure 1 shows that cynomolgus monkey intestine has multiple bands in the Western blot analysis using anti-MK2 antibody, suggesting the existence of several CES2 isoforms. The CL_{int} of cCES2 was higher than that of hCE2 for most substrates. Our results in this study demonstrated that recombinant hCE2 activities for most substrates were greater than those of mfCES2v3, which was in agreement with their intestinal hydrolysis. Interestingly, two amino acids important for substrate specificity are different in mfCES2v3 and cCES2; the 107th amino acid of cCES2 is Tyr, which is hydrophobic, compared with Gln in mfCES2v3, and cCES2 does not possess Met309. Furthermore, the total length of amino acids in cCES2 is the same as in hCE2 (559 amino acids), but different from mfCES2v3 (561 amino acids). Comparison of the substrate specificities of mfCES2v3 and cCES2 and their contributions to hydrolytic activities in cynomolgus monkey intestine will be examined once we have been able to produce recombinant cCES2 by cloning cCES2.

In addition, it was previously reported that intestinal hydrolysis shows no enantioselectivity toward propranolol derivatives in humans, rats, rabbits, and dogs,[21,41] with only monkey intestine showing enantioselective hydrolysis. CES2 isozymes are predominantly expressed in the intestine in most experimental animals, although dog intestine possesses no CES isozymes, but it seems that only monkey CES2 shows enantioselective hydrolysis of propranolol derivatives. Therefore, if in the future an esterified prodrug is developed to improve absorption, any data obtained using cynomolgus monkeys will need to be interpreted carefully if used to predict human intestinal absorption and metabolism. In this case, as described in the present study, the extent to which the substrate can be hydrolyzed by CES2 isozymes may be able to be predicted by homology modeling and docking simulation. Using this approach for each isozyme should increase our ability to extrapolate from laboratory animals to human disposition during pharmaceutical research and development. Further results using this approach, with other substrates and animal species, will be needed to promote and consolidate this field.

In conclusion, the *in vitro* study demonstrated that human intestine possesses higher hydrolytic activities for the substrates used in this study than monkey intestine and that substrate recognition is somewhat different between monkey and human systems, including *R*-preferential hydrolysis of propranolol derivatives in monkey intestine. This enantioselectivity appears to be derived from conformational flexibility in the active center of an intestinal monkey CES2 isozyme, with docking analysis suggesting that two amino acids around its active site influence these characteristics. Although it must be confirmed that the *in vitro* study based on standardized conditions accurately reflects the *in vivo* situation, these findings should help to illuminate the differences in intestinal hydrolytic activities between humans and cynomolgus monkeys and may be useful during drug development.

■ ASSOCIATED CONTENT

Supporting Information

The Supporting Information is available free of charge on the ACS Publications website at DOI: 10.1021/acs.molpharmaceut.6b00394.

Phylogenetic tree of CES2 isozymes, amino acid alignments used in the docking model, detailed structures of substrates used in this study, polyacrylamide gel electrophoresis of intestinal microsomes, and inhibitory effects of *O*-3-methyl-*n*-butyryl propranolol (PDF)

■ AUTHOR INFORMATION

Corresponding Author

*E-mail: iteruko@gpo.kumamoto-u.ac.jp. Tel/Fax: +81-96-371-4626.

Notes

The authors declare no competing financial interest.

■ ACKNOWLEDGMENTS

This research is partially supported by the Platform Project for Supporting in Drug Discovery and Life Science Research (Platform for Drug Discovery, Informatics and Structural Life Science) from the Ministry of Education, Culture, Sports, Science and Technology (MEXT), and the Japan Agency for Medical Research and Development (AMED).

DOI: 10.1021/acs.molpharmaceut.6b00394
Mol. Pharmaceutics 2016, 13, 3176−3186

REFERENCES

(1) Chiou, W. L.; Buehler, P. W. Comparison of oral absorption and bioavailability of drugs between monkey and human. *Pharm. Res.* **2002**, *19*, 868−74.

(2) Prueksaritanont, T.; Gorham, L. M.; Hochman, J. H.; Tran, L. O.; Vyas, K. P. Comparative studies of drug-metabolizing enzymes in dog, monkey, and human small intestines, and in Caco-2 cells. *Drug Metab. Dispos.* **1996**, *24*, 634−42.

(3) Kaji, H.; Kume, T. Glucuronidation of 2-(4-chlorophenyl)-5-(2-furyl)-4-oxazoleacetic acid (TA-1801A) in humans: species differences in liver and intestinal microsomes. *Drug Metab. Pharmacokinet.* **2005**, *20*, 206−11.

(4) Chu, X.; Bleasby, K.; Evers, R. Species differences in drug transporters and implications for translating preclinical findings to humans. *Expert Opin. Drug Metab. Toxicol.* **2013**, *9*, 237−52.

(5) Katoh, M.; Suzuyama, N.; Takeuchi, T.; Yoshitomi, S.; Asahi, S.; Yokoi, T. Kinetic analyses for species differences in P-glycoprotein-mediated drug transport. *J. Pharm. Sci.* **2006**, *95*, 2673−83.

(6) Takahashi, M.; Washio, T.; Suzuki, N.; Igeta, K.; Fujii, Y.; Hayashi, M.; Shirasaka, Y.; Yamashita, S. Characterization of gastrointestinal drug absorption in cynomolgus monkeys. *Mol. Pharmaceutics* **2008**, *5*, 340−8.

(7) Takai, S.; Matsuda, A.; Usami, Y.; Adachi, T.; Sugiyama, T.; Katagiri, Y.; Tatematsu, M.; Hirano, K. Hydrolytic profile for ester- or amide-linkage by carboxylesterase pI 5.3 and 4.5 from human liver. *Biol. Pharm. Bull.* **1997**, *20*, 869−73.

(8) Holmes, R. S.; Wright, M. W.; Laulederkind, S. J.; Cox, L. A.; Hosokawa, M.; Imai, T.; Ishibashi, S.; Lehner, R.; Miyazaki, M.; Perkins, E. J.; Potter, P. M.; Redinbo, M. R.; Robert, J.; Satoh, T.; Yamashita, T.; Yan, B.; Yokoi, T.; Zechner, R.; Maltais, L. J. Recommended nomenclature for five mammalian carboxylesterase gene families: human, mouse, and rat genes and proteins. *Mamm. Genome* **2010**, *21*, 427−41.

(9) Satoh, T.; Taylor, P.; Bosron, W. F.; Sanghani, S. P.; Hosokawa, M.; La Du, B. N. Current progress on esterases: from molecular structure to function. *Drug Metab. Dispos.* **2002**, *30*, 488−93.

(10) Satoh, T.; Hosokawa, M. The mammalian carboxylesterases: from molecules to functions. *Annu. Rev. Pharmacol. Toxicol.* **1998**, *38*, 257−88.

(11) Satoh, T.; Hosokawa, M. Structure, function and regulation of carboxylesterases. *Chem.-Biol. Interact.* **2006**, *162*, 195−211.

(12) Xu, G.; Zhang, W.; Ma, M. K.; McLeod, H. L. Human carboxylesterase 2 is commonly expressed in tumor tissue and is correlated with activation of irinotecan. *Clin. Cancer Res.* **2002**, *8*, 2605−11.

(13) Williams, E. T.; Jones, K. O.; Ponsler, G. D.; Lowery, S. M.; Perkins, E. J.; Wrighton, S. A.; Ruterbories, K. J.; Kazui, M.; Farid, N. A. The biotransformation of prasugrel, a new thienopyridine prodrug, by the human carboxylesterases 1 and 2. *Drug Metab. Dispos.* **2008**, *36*, 1227−32.

(14) Imai, T. Human carboxylesterase isozymes: catalytic properties and rational drug design. *Drug Metab. Pharmacokinet.* **2006**, *21*, 173−85.

(15) Laizure, S. C.; Herring, V.; Hu, Z.; Witbrodt, K.; Parker, R. B. The role of human carboxylesterases in drug metabolism: have we overlooked their importance? *Pharmacotherapy* **2013**, *33*, 210−22.

(16) Taketani, M.; Shii, M.; Ohura, K.; Ninomiya, S.; Imai, T. Carboxylesterase in the liver and small intestine of experimental animals and human. *Life Sci.* **2007**, *81*, 924−32.

(17) Williams, E. T.; Wang, H.; Wrighton, S. A.; Qian, Y. W.; Perkins, E. J. Genomic analysis of the carboxylesterases: identification and classification of novel forms. *Mol. Phylogenet. Evol.* **2010**, *57*, 23−34.

(18) Williams, E. T.; Bacon, J. A.; Bender, D. M.; Lowinger, J. J.; Guo, W. K.; Ehsani, M. E.; Wang, X.; Wang, H.; Qian, Y. W.; Ruterbories, K. J.; Wrighton, S. A.; Perkins, E. J. Characterization of the expression and activity of carboxylesterases 1 and 2 from the beagle dog, cynomolgus monkey, and human. *Drug Metab. Dispos.* **2011**, *39*, 2305−13.

(19) Uno, Y.; Uehara, S.; Hosokawa, M.; Imai, T. Systematic identification and characterization of carboxylesterases in cynomolgus macaques. *Drug Metab. Dispos.* **2014**, *42*, 2002−6.

(20) Hosokawa, M.; Maki, T.; Satoh, T. Characterization of molecular species of liver microsomal carboxylesterases of several animal species and humans. *Arch. Biochem. Biophys.* **1990**, *277*, 219−27.

(21) Imai, T.; Taketani, M.; Shii, M.; Hosokawa, M.; Chiba, K. Substrate specificity of carboxylesterase isozymes and their contribution to hydrolase activity in human liver and small intestine. *Drug Metab. Dispos.* **2006**, *34*, 1734−41.

(22) Uno, Y.; Fujino, H.; Kito, G.; Kamataki, T.; Nagata, R. CYP2C76, a novel cytochrome P450 in cynomolgus monkey, is a major CYP2C in liver, metabolizing tolbutamide and testosterone. *Mol. Pharmacol.* **2006**, *70*, 477−86.

(23) Ohura, K.; Nakada, Y.; Kotani, S.; Imai, T. Design of fexofenadine prodrugs based on tissue-specific esterase activity and their dissimilar recognition by P-glycoprotein. *J. Pharm. Sci.* **2015**, *104*, 3076−83.

(24) Bradford, M. M. A rapid and sensitive method for the quantitation of microgram quantities of protein utilizing the principle of protein-dye binding. *Anal. Biochem.* **1976**, *72*, 248−54.

(25) Liu, Y.; Patricelli, M. P.; Cravatt, B. F. Activity-based protein profiling: the serine hydrolases. *Proc. Natl. Acad. Sci. U. S. A.* **1999**, *96*, 14694−9.

(26) Yamaoka, K.; Tanigawara, Y.; Nakagawa, T.; Uno, T. A pharmacokinetic analysis program (multi) for microcomputer. *J. Pharmacobio-Dyn.* **1981**, *4*, 879−85.

(27) Bencharit, S.; Edwards, C. C.; Morton, C. L.; Howard-Williams, E. L.; Kuhn, P.; Potter, P. M.; Redinbo, M. R. Multisite promiscuity in the processing of endogenous substrates by human carboxylesterase 1. *J. Mol. Biol.* **2006**, *363*, 201−14.

(28) Friesner, R. A.; Banks, J. L.; Murphy, R. B.; Halgren, T. A.; Klicic, J. J.; Mainz, D. T.; Repasky, M. P.; Knoll, E. H.; Shelley, M.; Perry, J. K.; Shaw, D. E.; Francis, P.; Shenkin, P. S. Glide: A new approach for rapid, accurate docking and scoring. 1. Method and assessment of docking accuracy. *J. Med. Chem.* **2004**, *47*, 1739−49.

(29) Bowers, K. J.; Chow, D. E.; Xu, H.; Dror, R. O.; Eastwood, M. P.; Gregersen, B. A.; Klepeis, J. L.; Kolossvary, I.; Moraes, M. A.; Sacerdoti, F. D.; Salmon, J. K.; Shan, Y.; Shaw, D. E. Scalable algorithms for molecular dynamics simulations on commodity clusters. Proceeding SC '06 Proceedings of the 2006 ACM/IEEE Conference on Supercomputing Article No. 84; ACM: New York, 2006. DOI: 10.1145/1188455.1188544.

(30) Imai, T.; Ohura, K. The role of intestinal carboxylesterase in the oral absorption of prodrugs. *Curr. Drug Metab.* **2010**, *11*, 793−805.

(31) Block, W.; Arndt, R. Chromatographic study on the specificity of bis-p-nitrophenylphosphate in vivo. Identification of labelled proteins of rat liver after intravenous injection of bis-p-nitro[14C]-phenylphosphate as carboxylesterases and amidases. *Biochim. Biophys. Acta* **1978**, *524*, 85−93.

(32) Hosokawa, M. Structure and catalytic properties of carboxylesterase isozymes involved in metabolic activation of prodrugs. *Molecules* **2008**, *13*, 412−31.

(33) Ishizuka, T.; Fujimori, I.; Kato, M.; Noji-Sakikawa, C.; Saito, M.; Yoshigae, Y.; Kubota, K.; Kurihara, A.; Izumi, T.; Ikeda, T.; Okazaki, O. Human carboxymethylenebutenolidase as a bioactivating hydrolase of olmesartan medoxomil in liver and intestine. *J. Biol. Chem.* **2010**, *285*, 11892−902.

(34) Bencharit, S.; Morton, C. L.; Howard-Williams, E. L.; Danks, M. K.; Potter, P. M.; Redinbo, M. R. Structural insights into CPT-11 activation by mammalian carboxylesterases. *Nat. Struct. Biol.* **2002**, *9*, 337−42.

(35) Bencharit, S.; Morton, C. L.; Hyatt, J. L.; Kuhn, P.; Danks, M. K.; Potter, P. M.; Redinbo, M. R. Crystal structure of human carboxylesterase 1 complexed with the Alzheimer's drug tacrine: from binding promiscuity to selective inhibition. *Chem. Biol.* **2003**, *10*, 341−9.

DOI: 10.1021/acs.molpharmaceut.6b00394
Mol. Pharmaceutics 2016, 13, 3176−3186

(36) Bencharit, S.; Morton, C. L.; Xue, Y.; Potter, P. M.; Redinbo, M. R. Structural basis of heroin and cocaine metabolism by a promiscuous human drug-processing enzyme. *Nat. Struct. Biol.* **2003**, *10*, 349−56.
(37) Fleming, C. D.; Bencharit, S.; Edwards, C. C.; Hyatt, J. L.; Tsurkan, L.; Bai, F.; Fraga, C.; Morton, C. L.; Howard-Williams, E. L.; Potter, P. M.; Redinbo, M. R. Structural insights into drug processing by human carboxylesterase 1: tamoxifen, mevastatin, and inhibition by benzil. *J. Mol. Biol.* **2005**, *352*, 165−77.
(38) Hemmert, A. C.; Otto, T. C.; Wierdl, M.; Edwards, C. C.; Fleming, C. D.; MacDonald, M.; Cashman, J. R.; Potter, P. M.; Cerasoli, D. M.; Redinbo, M. R. Human carboxylesterase 1 stereoselectively binds the nerve agent cyclosarin and spontaneously hydrolyzes the nerve agent sarin. *Mol. Pharmacol.* **2010**, *77*, 508−16.
(39) Wierdl, M.; Tsurkan, L.; Hyatt, J. L.; Edwards, C. C.; Hatfield, M. J.; Morton, C. L.; Houghton, P. J.; Danks, M. K.; Redinbo, M. R.; Potter, P. M. An improved human carboxylesterase for enzyme/prodrug therapy with CPT-11. *Cancer Gene Ther.* **2008**, *15*, 183−92.
(40) Vistoli, G.; Pedretti, A.; Mazzolari, A.; Testa, B. Homology modeling and metabolism prediction of human carboxylesterase-2 using docking analyses by GriDock: a parallelized tool based on AutoDock 4.0. *J. Comput.-Aided Mol. Des.* **2010**, *24*, 771−87.
(41) Yoshigae, Y.; Imai, T.; Horita, A.; Matsukane, H.; Otagiri, M. Species differences in stereoselective hydrolase activity in intestinal mucosa. *Pharm. Res.* **1998**, *15*, 626−31.

DOI: 10.1021/acs.molpharmaceut.6b00394
Mol. Pharmaceutics 2016, 13, 3176−3186